A fine discrete field cellular automaton for pedestrian dynamics integrating pedestrian heterogeneity, anisotropy, and time-dependent characteristics

Article *in* Transportation Research Part C Emerging Technologies · April 2018

DOI: 10.1016/j.trc.2018.03.022

CITATIONS
52

READS
374

6 authors, including:

Zhijian Fu
Southwest Jiaotong University
38 PUBLICATIONS **613** CITATIONS

SEE PROFILE

Jian Ma
Southwest Jiaotong University
98 PUBLICATIONS **2,024** CITATIONS

SEE PROFILE

Ke Han
Southwest Jiaotong University
143 PUBLICATIONS **2,282** CITATIONS

SEE PROFILE

A Fine Discrete Field Cellular Automaton for Pedestrian Dynamics Integrating Pedestrian Heterogeneity, Anisotropy, and Time-Dependent Characteristics

Zhijian Fu[a], Qihao Jia[a], Junmin Chen[b], Jian Ma[a], Ke Han[c,1], Lin Luo[d,2]

[a] School of Transportation and Logistics, Southwest Jiaotong University, Chengdu, 610031, PRC
[b] Faculty of Geosciences and Environmental Engineering, Southwest Jiaotong University, Chengdu, 610031, PRC
[c] Department of Civil and Environmental Engineering, Imperial College London, London SW7 2BU, UK
[d] State Key Laboratory of Fire Science, University of Science and Technology of China, Hefei, 230026, PRC

Abstract

This paper proposes a discrete field *cellular automaton* (CA) model that integrates pedestrian heterogeneity, anisotropy, and time-dependent characteristics. The pedestrian movement direction, moving/staying, and steering are governed by the *transfer equations*. Compared with existing studies on fine-discretized CA models, the proposed model is advantageous in terms of flexibility, higher spatial accuracy, wider speed range, relatively low computational cost, and elaborated conflict resolution with synchronous update scheme. Three different application scenarios are created by adjusting the definite conditions of the model: (1) The first one is a unidirectional pedestrian movement in a channel, where a complete jam in the high-density region is observed from the proposed model, which is missing from existing floor field CA models. (2) The second one is evacuation from a room, where the evacuation time is independent of the discretization factor, which is different from previous work. (3) The third one is an ascending evacuation through a 21-storey stair system, where pedestrians move with constant speed or with fatigue. The evacuation time in the latter case is nearly twice of that in the former.

Keywords: Heterogeneity, Anisotropy, Time-dependent Characteristics, Discretization, Transfer equations, Definite conditions

1. Introduction

The accurate and realistic modeling of pedestrian movement is essential for the efficient and safe flow of pedestrians. Application scenarios include, but are not limited to, planning of pedestrian facilities, prevention of crowd disaster, and optimization of evacuation routes. Pedestrian heterogeneity, anisotropy and time-dependent characteristics may play dominant roles

[1] Corresponding author, e-mail: k.han@imperial.ac.uk, tel.: +44 (0)20-7594-5682
[2] Corresponding author, e-mail: luolin09@mail.ustc.edu.cn

on the modeling of pedestrian dynamics. Some well-known examples are as follows.

(1) Pedestrian traffic is physiologically heterogeneous in terms of age, gender, incapacitation, and psychological characteristics (e.g. perception and reflection of the surrounding environment) (Fu et al. 2015a, Fu et al. 2015b);

(2) The physical size and behavior of a pedestrian in different directions is varied, i.e., anisotropy. For example, pedestrians react mainly to stimuli in front of them (Kirchner et al. 2004). Additionally, the free speeds of walking forward, laterally, and backward are different, which is modeled as a specific kind of behavior termed *sidestepping* in this paper.

(3) Parameters of pedestrian movement may change with time. Examples include fatigue (Luo et al. 2016), falling and injury. Usually, a pedestrian adjusts continuously his/her velocity to the surrounding pedestrian density, a phenomenon quantified by the fundamental diagram (Seyfried et al. 2005; Seyfried et al. 2009).

Numerous models for pedestrian dynamics have been proposed so far, and can be categorized as macroscopic/microscopic or discrete/continuous (Schadschneider et al. 2011). The three key theoretical and practical criteria against which a pedestrian model is evaluated are:

(1) How to realistically model pedestrian movement using some relatively simple rules or equations (Moussaïd et al. 2011);

(2) How to easily extend the general model to simulate specific pedestrian movement (such as evacuation from a complex structure building) by adding/removing or modifying definite conditions; and

(3) How to efficiently conduct large-scale crowd simulation with acceptable errors.

As one type of microscopic discrete model, traditional *floor field cellular automaton* (FFCA) model enjoys flexibility, extendibility and computational efficiency (Burstedde et al. 2001). It has successfully reproduced many self-organization collective phenomena (Helbing et al. 2001), such as jamming and clogging, lane formation, and oscillation at bottlenecks. However, like many other grid-based models, *cellular automaton* (CA) models are often criticized for the over-discretization of space and time (Pelechano and Malkawi 2008, Liu et al. 2014a), resulting in unrealistic pedestrian movement such as diagonal movement trajectories and limited speed range.

In most CA models, each pedestrian occupies exactly one cell and moves through one cell per time step. It is a finite approximation of the reality. According to Kirchner et al. (2004) and Guo (2014), a fine (spatial) discretization can enable: (1) an easy implementation of realistic velocity distribution; (2) accurate geometric structure of pedestrian facilities; (3) analysis in relation to continuous models; (4) characterization of specific phenomena such as dead-lock and misalignment; (5) quantitative analysis and calibration of pedestrian dynamic models; and (6) modeling of pedestrian anisotropy.

A number of fine discrete models have been proposed in the literature. Kirchner et al. (2004) first investigate the discretization effect, and find that the fundamental diagram with pedestrians velocity $v_{max}>1$ (grid/time step) fits better with empirical results than $v_{max}=1$ (grid/time step). In Kirchner's model, a $0.4m\times0.4m$ square, which is the projection area of a pedestrian from empirical observation, is divided into 2×2 grids, and the pedestrian desired velocity is a multiple of $1.3m/s$. In many cases this coarse discretization does not yield accurate results, and finer grids combined with continuously varying velocity are needed. Song et al. (2006) introduce interaction forces, and allow overlaps among pedestrians. In their 3×3 grid model, every pedestrian has the same desired velocity ($1m/s$). However, this model lacks flexibility and computational efficiency when used in

some complex pedestrian traffic scenarios. For example, in counter flow, the 'cores' of several pedestrians might collide with each other because of the forces. Weng et al. (2007) consider smaller spatial grids but again assuming that all the pedestrians have the same desired velocity, which is a multiple of $0.25m/s$. This results in unrealistic coarse trajectories. With finer spatial and temporal discretization, Xu et al. (2008) propose a discrete model where the desired velocity is $1m/s$, and the distance traveled by a pedestrian is a multiple of the grid size (which is equal to the size of a pedestrian). As a consequence, in their model pedestrians always align with each other, leading to unrealistically high efficiency in evacuation scenarios. Zhang et al. (2008) stipulate that a pedestrian moves according to the free movement velocity and the unoccupied space in his/her moving direction; this yields the phenomena of monopolizing exit and dislocable queues. However, the velocity rule tends to generate coarse, unrealistic zig-zag trajectories of pedestrians. Considering contact forces among pedestrians, Guo and Huang (2008) model push and bump with a pedestrian occupying 3×3 grids by a modified floor field CA model. Later, under both good and zero visibility conditions, Guo et al. (2012) study evacuation from a classroom with a pedestrian occupying 2×2 grids. In these two models, however, pedestrians have the same desired free velocity. Even though finer discretization is proposed in another work (Guo, 2014), pedestrians in the model still have the same desired free velocity of $1m/s$. The transfer probabilities of directions are calculable only for a specific structure (i.e. a square room), and cannot be applied to more complex building structures. Furthermore, pedestrians move in a single direction in one time step, resulting in unrealistic formation of crowds around the exit.

One should also note that for most of these aforementioned finer discrete models, shuffled or sequential update scheme is used. However, for sequential scheme, pedestrians are not equal-footing, and the results might be quite different depending on the sequences. Schadschneider and Seyfried (2009) believed that both shuffled and sequential schemes are difficult to calibrate (e.g. in reality, pedestrians always make decisions at the same time but not in any order), and appear to be rather unrealistic. Besides, Kirchner et al. (2003) argued that any other form of random or ordered sequential update schemes tends to disguise the real number of conflicts arising among pedestrians in the system. In reality, pedestrians in conflict situations slow down or hesitate for a short moment when trying to resolve the conflict. This reduces, on average, the velocity of all pedestrians involved. In some cases, for example evacuation of a room, the modifications of the update schemes make the models behave in different ways (Seitz and Köster, 2014). Xu et al. (2008) found that the update schemes have significant influence on the evacuation time when analyzing the discretization effect in FFCA model. Kirchner et al. (2004) pointed out that the evolution of flow rate changes with different update schemes. Most recently, Luo et al. (2018) investigated the influence of four different update schemes on pedestrian dynamics in a quantitative and systematic way. They found that for pedestrian evacuation, the evacuation time is enlarged, and the difference in pedestrians' walking abilities are better reflected, under parallel scheme. In face of a bottleneck, using a parallel scheme leads to a longer congestion period and a more dispersive density distribution. The exit flow and space-time distribution of density and velocity have significant discrepancies under different schemes when pedestrian flow with high desired velocity is simulated.

Thus, for the purpose of calibration and capturing conflicts, a synchronous/parallel update scheme is preferred. However, the complex conflict resolution due to fine discretization has to be taken into consideration as one employs a synchronous/parallel update scheme.

In summary, the main drawbacks of the studies reviewed above include: (1) limited accuracy with low speed increment and narrow speed range, relative coarse pedestrian trajectories, and rough spatial discretization of pedestrian facilities; (2) limited extension for simulating complex scenarios with low computational cost; and (3) overlooking conflicts among pedestrians by using instead shuffled or sequential update schemes.

Aiming to tackle these three challenges, and simultaneously capture pedestrian heterogeneity, partial anisotropy and time-dependent characteristics, this paper proposes a refined discrete floor field CA model where a pedestrian occupies multiple grids (in traditional CA models, a pedestrian occupies exactly one grid), and the time step is equal to the ratio of spatial step and the maximum desired velocity. Our modeling framework consists of two parts: Model formulation and solution approaches.

The model formulation includes:

(1) Basic assumptions regarding physical analogy, for example, treating pedestrians as fluids (Hughes 2002) or self-driven agents (Vicsek and Zafeiris 2012), and the exclusion principal;

(2) Transfer equations that determine transfer probability governing pedestrian movement and steering; and

(3) Definite conditions including boundary conditions, initial conditions, and specific pedestrians characteristics (e.g. disability, gender, and specific pedestrian behaviors such as separation, alignment, cohesion, overtaking, fatigue, following a leader, and communications).

The solution approach includes:

(1) Discretization methods for space, time and and pedestrian state;

(2) Conflict resolution methods; and

(3) Update schemes.

Compared with CA models in the literature that almost only perform fine spatial discretization, the proposed model makes contributions in the following regards.

(1) **Flexibility and extendibility**. The proposed model is easy to be extended to treat pedestrian traffic with different behaviors in a complex environment, by adding/modifying some definite conditions. Complex environment and social relationship could be incorporated into the static and dynamic field of information. Additionally, almost all characteristics and behaviors of the pedestrian can be physically reflected by the pedestrian speed and angular velocity. (See an example in Sec. 3.3)

(2) **Higher spatial accuracy spatial**. Firstly, compared with traditional CA models, the space is fine discretized; i.e. the spatial unit can be much smaller than the scale of a pedestrian. Thus, details of small or irregular geometrical structures can be easily represented, unlike most existing discrete models. Secondly, in previous work, most discrete models stipulate that pedestrians walk across several grids per time interval, to realize a velocity greater than one (Guo 2014; Weng et al. 2007; Xu et al. 2008; Zhang et al. 2008). This causes undesirable alignments and coarse zig-zag trajectories, while those problems can be avoided in our model by just making each pedestrian walk at most one grid per time interval. Thus, some specific phenomena such as dead-lock and misalignment can be reproduced in our model.

(3) **Wider speed range.** Compared with previous discrete models where the desired velocity takes on only a few specific values, the desired velocity in our model can be continuously varying according to internal or external conditions, without ad hoc upper and lower bounds. Consequently,

for a heterogeneous crowd, phenomena like fatigue, injury, and overtaking can be easily modeled.

(4) **Low computational cost.** The desired velocity (including angular velocity) in the proposed model is decoupled into direction, modulus, and angular speed. The *transfer probability* governing pedestrian movement is decoupled into *transfer probability* of direction, speed, and angular speed. For a speed increment of 0.1m/s, previous models with fine spatial discretization (e.g. Kirchner et al. 2004) need to use at least 10 time steps to realize a speed larger than 1m/s, whereas our model only requires 1 time step. If the pedestrian reaches a speed greater than 1m/s, a time step in existing models has to be divided into several sub-steps, and conflicts should be resolved in each sub-step, which is quite complex and time consuming. In contrast, such division of one time step is no longer needed in our model.

(5) **Elaborated conflict resolution**. Unlike those previous CA models with fine spatial discretization, which usually ignore conflicts among pedestrians by shuffled update schemes, this paper treats conflicts using the synchronous update scheme based on a good understanding of the nature of the conflict (Luo et al. 2018). This is done by introducing a detailed competitive relationship among individuals and the average competitive capacity of individuals involved in the conflicts (Fu et al. 2015b).

The rest of the paper is organized as follows. Section 2 elaborates the modeling framework and its solution procedure. In Section 3, we demonstrate and analyze the key features of the proposed model via three case studies: pedestrian flow through a channel (Section 3.1.), evacuation from a single room (Section 3.2.), and evacuation from a 21-storey stair (Section 3.3.). Section 4 gives a further discussion. Finally, Section 5 provides some concluding remarks.

2. Model Development

The following two basic assumptions are made, which are easily verifiable with real-world observations.

Assumption 1. Pedestrians are physically analogized as intelligent agents who evaluate the surrounding environment and change their walking properties.

Assumption 2. (Exclusion principle). Each pedestrian occupies a certain place. Any form of overlapping is forbidden.

2.1. Transfer Equation and Discretization

Pedestrians' movement and steering are governed by the so-called *transfer probabilities*, which are determined by *transfer equations*. Unlike the transfer equation in most floor field CA models where only the transfer probability regarding direction is taken into account (e.g. Burstedde et al. 2001), the transfer equation in the proposed model considers not only the transfer probability regarding direction but also the transfer probabilities regarding speed and steering.

In a Cartesian coordinate, without considering steering the transfer equation can be simply expressed as

$$\frac{\mathrm{d}r\left(t\right)}{\mathrm{d}t}=v\left(t\right) \tag{1}$$

where $r(t)$ is the pedestrian position, $v(t)$ is the desired velocity which can be decoupled into the direction $\lambda(t)$ and the modulus/desired speed $\|v(t)\|$ (Moussaïd et al. 2011). Eq.(1) can be discretized into

$$\Delta r(t) = r(t+\Delta t) - r(t) = \lambda(t) \cdot \|v(t)\| \cdot \Delta t \tag{2}$$

where Δt is a time step.

According to Weidmann (1992), the empirically observed maximum density is about 6.25*ped*·*m*$^{-2}$. Usually a pedestrian is assumed to occupy a 0.4*m*×0.4*m* square in many literatures (Weidmann 1992; Burstedde et al. 2001), which corresponds to the vertical projection of an individual on the floor. However, according to the statistics of human dimensions of Chinese adults (National Standard of People's Republic of China, GB-10000-88, 1988), the width of an adult is almost twice of the depth. The physical scales of a pedestrian in different directions are not the same. Thus, in this paper, two kinds of pedestrian physical sizes are considered, namely 0.4*m*×0.4*m* square and 0.4*m*×0.2*m* rectangle (Zhu et al. 2017). The length scale of finer discrete space is *a*=(0.4/*n*) *m*, which means that a pedestrian occupies *n*×*n* grids or *n*×*n*/2 grids, where *n* is defined as the discretization factor.

The time step can be determined as,

$$\Delta t = \frac{a}{v_{\max}} \tag{3}$$

where $v_{\max}$ is the maximum desired speed of the pedestrian system.

Thus, combining Eqns (2) and (3), we have

$$\frac{\Delta r(t)}{a} = \lambda(t) \cdot \frac{\|v(t)\|}{v_{\max}} \tag{4}$$

2.1.1. Transfer Equation Governing Movement Direction $\lambda(t)$

According to **Assumption 1**, pedestrians are modeled as intelligent agents, who can make their decisions of movement and rotation directions according to the superposition of *static field S* and *dynamic field D* (Burstedde et al. 2001). As for the movement direction, the *transfer probability* to the direction *i* (forward, rightward, leftward, backward, or stay) is given by,

$$P\left[\lambda(t) = \lambda_i\right] = N \exp\left[\frac{\sum_{j=1}^{b}\left(K_S \cdot S_j + K_D \cdot D_j\right)}{b}\right] \cdot \varepsilon_i, \quad \left(b = n^2 \text{ or } b = n^2/2\right) \tag{5}$$

where

N is the normalized factor to make sure that the sum of transfer probabilities in all the directions is one;

j is the expecting grids to be occupied by the pedestrian in the next time step;

b equals n^2 if the pedestrian occupies *n*×*n* grids (the projection of a pedestrian is treated as a

square), or equals $n^2/2$ if the pedestrian occupies $n \times n/2$ grids (the projection of a pedestrian is treated as a rectangle);

ε reflects the influence of obstacles. It takes 0 if any neighbors in the expected movement direction is occupied by obstacles or pedestrians, i.e., the exclusion principle;

K_S and K_D are sensitivity parameters of static field and dynamic field, respectively. As K_S increases, pedestrians become more familiar with the static environment. As K_D increases, the interactions between pedestrians and the effect of changing environment become strong.

The *static field S* does not vary with time (i.e., $\frac{\partial S}{\partial t} = 0$). It is generated by the static environment (e.g. exits and obstacles). Usually the static field of fixed geometry structures is iterated from each exit, and a kind of iteration rule can be found in (Fu et al. 2013). The dynamic field is regarded as interactions between pedestrians and the influence of changing environment, and varies with time (i.e., $\frac{\partial D}{\partial t} \neq 0$). In Burstedde et al. (2001), the dynamic field is virtual trace left by pedestrians with decay α and diffusion β.

$$\frac{\partial D}{\partial t} = \alpha \cdot \Delta D - \beta \cdot D \tag{6}$$

2.1.2. *Transfer Equation Governing Moving or Staying* $\frac{\|v(t)\|}{v_{\max}}$

According to Helbing et al. (2005), pedestrians' free velocity follows Gaussian distribution, and can be expressed as $v_f \quad N\left(1.34, 0.34^2\right)$, which also means that pedestrians have different walking abilities. Moreover, the velocity of a pedestrian continuously changes to adapt to the changing environment. Thus, as for the velocity modulus in the right part of eq.(4), the *transfer probabilities* to move and stop are respectively determined as

$$P\left(\frac{\|v(t)\|}{v_{\max}} \coloneqq 1\right) = \frac{\|v(t)\|}{v_{\max}}, \quad P\left(\frac{\|v(t)\|}{v_{\max}} \coloneqq 0\right) = 1 - \frac{\|v(t)\|}{v_{\max}} \tag{7}$$

which means that in every time step the pedestrian has a probability of $\frac{\|v(t)\|}{v_{\max}}$ to move.

2.1.3. *Transfer Equations Governing Steering*

Pedestrians often move with changing their orientations $o(t)$ to a preferred direction $\lambda_{\max}(t)$ with the highest field, namely steering, as illustrated in fig.1. We name the angle between the orientation and the abscissa as θ. Then,

$$\begin{aligned} \Delta o(t) &= \left[\cos\theta(t+\Delta t) - \cos\theta(t), \sin\theta(t+\Delta t) - \sin\theta(t)\right] \\ &= \left[\cos\left(\theta(t) + \Delta\theta(t)\right) - \cos\theta(t), \sin\left(\theta(t) + \Delta\theta(t)\right) - \sin\theta(t)\right] \\ &= \left[\cos\left(\theta(t) + \omega(t)\cdot\Delta t\right) - \cos\theta(t), \sin\left(\theta(t) + \omega(t)\cdot\Delta t\right) - \sin\theta(t)\right] \end{aligned} \tag{8}$$

where ω is the pedestrian angular speed.

If in every time step, a pedestrian can rotate with an angle up to $\pi/2$. Then, the transfer probability to steer can be given as,

$$\begin{cases} P_S = 2\omega(t)\cdot\Delta t/\pi & (\omega(t)\cdot\Delta t \le \pi/2) \\ 1 & (\omega(t)\cdot\Delta t > \pi/2) \end{cases} \tag{9}$$

For simplicity, we can also assign the *transfer probability* to steer P_S as a constant. Then, the rotation angular in a time step is given as,

$$\Delta o(t) = \begin{cases} 0 & \left(\varphi > P_S \vee o(t) = \lambda_{\max}(t)\right) \\ \lambda_{\max}(t) - o(t) & \left(\varphi \le P_S \wedge o(t) \ne \lambda_{\max}(t)\right) \end{cases} \tag{10}$$

where φ is a pseudo random number with $0 \le \varphi \le 1$.

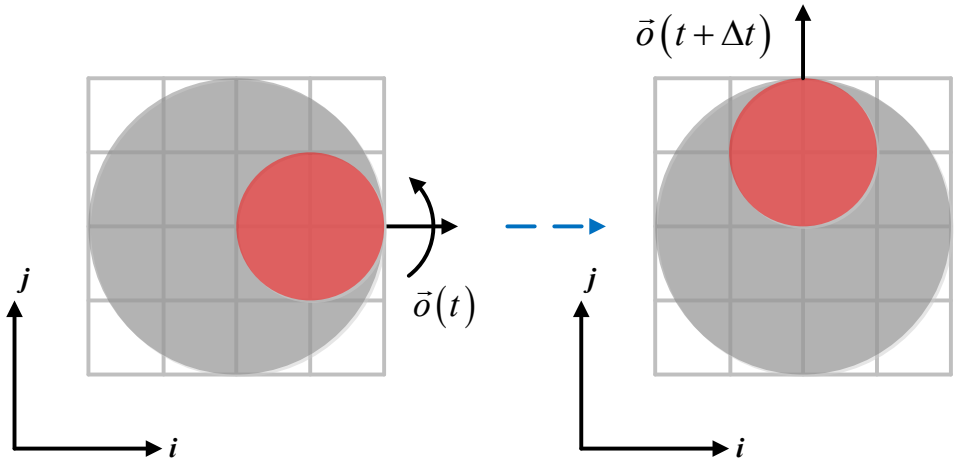

Fig. 1. Steering Behavior. Red circles are heads of a pedestrian, and the pedestrian changes his orientation from the right to the up

In every time step, a pedestrian makes decision to move or/and steer. In the condition that the pedestrian does not move and steer at the same time step, eq. (4) is changed to

$$\frac{\Delta r(t)}{a} = \delta\cdot\lambda(t)\cdot\frac{\|v(t)\|}{v_{\max}} \tag{11}$$

where

$$\delta = \begin{cases} 1 & \left(\Delta o(t) = 0\right) \\ 0 & \left(\Delta o(t) \ne 0\right) \end{cases} \tag{12}$$

2.2. Definite Conditions

Definite conditions are constraints of the transfer equations, which determine the *static field S*, the *dynamic field D*, the pedestrian desire speed $\|v(t)\|$, angular velocity ω, and then the transfer probabilities. They include boundary conditions, initial conditions, pedestrian specific behavior

and characteristics.

(1) Boundary Conditions

Boundary conditions are the static field and dynamic field at the boundaries of geometric structures, e.g., at the walls, exits, and/or obstacles.

The static field in the positions of walls and obstacles is 0, i.e., $S_W = 0$, while the static field in the positions of exits is set to be the maximum. By iteration rules as mentioned above in Section 2.1, the static field of the whole space is generated.

The changing environment such as the spreading fire or smoke, movable obstacles and social relationship between pedestrians determine the *dynamic field D* which is a function of the initial dynamic field D_0 and the time t.

$$D = f\left(D_0, t\right) \tag{13}$$

where the sophisticated function or rule f is usually determined through empirical results from previous studies and experiments.

For instance, the dynamic field of the following traces with diffusion and decay can be denoted as eq. (6) with the initial dynamic field distribution $D_0(x,y,t_0)=0$. The dynamic field increases by one in the positions where pedestrians leave in every time step. For the positions that are occupied by movable obstacles, the *dynamic field* can be formulated as

$$D_m\left(t\right) = -\frac{K_S \cdot S}{K_D} \tag{14}$$

(2) Initial Conditions

Initial conditions give the initial distribution of dynamic field $D_0(x,y,t_0)$, which relates to, for example, the initial distributions of pedestrians, the initial distributions of hazards, and movable obstacles. Based on both boundary conditions and initial conditions, we can draw the *field map*, which determines transfer equations regarding the movement direction and the orientation direction.

(3) Specific Behavior and Characteristics

Typical characteristics of pedestrians include age, gender, physical size, and disability, which might influence the pedestrians' walking properties. Specific behaviors are, for example, steering, herding, following a leader, fatigue, and communication among pedestrians. Almost all these characteristics and behaviors can be reflected by pedestrian speed $\left\|v\left(t\right)\right\|$ and angular velocity ω. For example, in this paper, sidestepping behavior is considered. Free speed of lateral movement and backward movement are 1/2 and 1/3 of the free speed of forward movement, i.e., $\left\|v\left(t\right)\right\| = \frac{v_f}{2}, \frac{v_f}{3}$ for lateral movement and backward movement respectively.

2.3. Conflict Resolution

In this paper, pedestrians only react to the environment of the current time step, and do not evaluate grids states of the next time step. As shown in Fig.2, the only feasible direction for pedestrian *A* in the next time step is upward due to the hard-core exclusion principle, since his/her neighboring cell on the right are partially occupied by the pedestrian *B*. The phenomenon that pedestrian *A* and Pedestrian *B* move rightward in the same time step is called as 'lock-step' or step synchronization, which enhances the pedestrian traffic efficiency especially in high density region (Fu et al. 2015a).

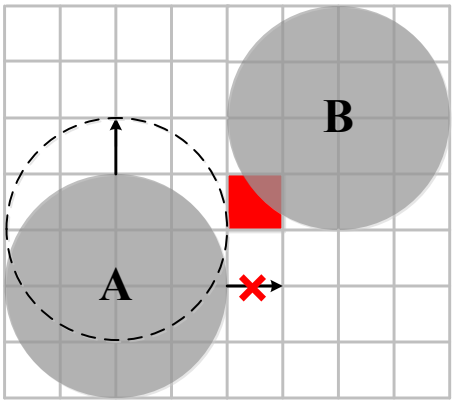

Fig. 2. Hard-core exclusion principle, any parts of overlapping is forbidden

Since the exclusion principle and synchronous update scheme are used, conflicts should be considered when pedestrians compete for the same target cells. In traditional CA models, conflicts can be regarded as local interactions (fig. 3(a)), because only a small number of pedestrians can access the same target cell, which is determined by the coordinate number of the target cell (Kirchner et al. 2004). As for finer discrete models, conflicts are not local anymore. Conflicts are not restricted to single cells and can spread over a wider area (fig. 3(b)). A pedestrian involves conflicts with at most two other pedestrians, and a cell can be the target for at most two pedestrians under this situation.

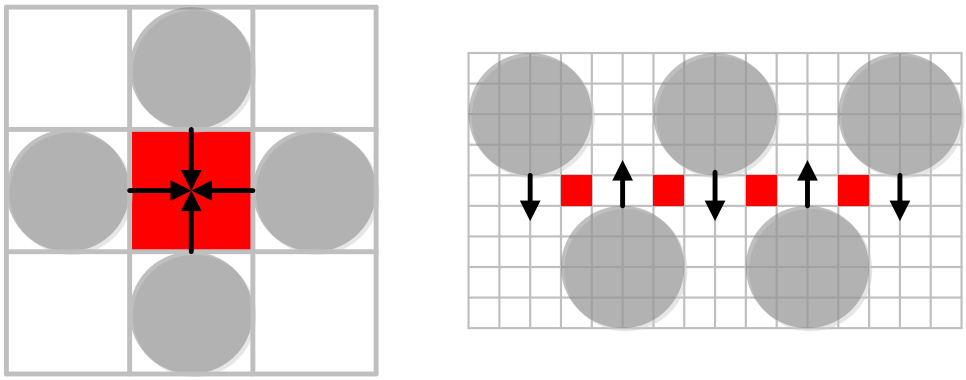

(a) (b)

Fig. 3. Conflicts among pedestrians with (a) n=1, and (b) n=4. The red cells are the target space more than one pedestrians compete for.

Based on the intuitive understanding of conflict, usually, pedestrians with higher velocity are

more unpleasant to stop suddenly. So they more likely tend to compete with each other, rather than to cooperate with each other. Then, the friction factor which is the probability that none of conflict involving pedestrians succeeds in accessing the target position can be assumed as,

$$\mu = \left(\langle v \rangle / v_{\inf} \right)^m \tag{15}$$

where $\langle v \rangle$ is the average speed of pedestrian involving conflict, and $v_{\inf}$ is the maximum desired speed that a pedestrian can reach, here $5m/s$ closing to the running speed of pedestrian. Pedestrians with high desired velocity close to $v_{\inf}$ seems to block themselves due to the high friction. m reflects the competition relationship between individuals. As m=0, individuals compete with each other completely, i.e., none of pedestrians involving conflict can reach the target cells. As $m \to \infty$, individuals cooperate with each other completely, i.e., one of them can reach his/her targets.

Since pedestrian with high desired velocity usually have a strong aggression, the probability of pedestrian i succeeding in competing is,

$$\mu = \left\| v_i \right\|^k / \sum_i \left\| v_i \right\|^k \tag{16}$$

where k reflects the average competitive capacity of pedestrians involving conflicts. As k=0, pedestrians involving conflict with different desired velocity have the same competitive capacity. With $k \to \infty$, only pedestrians with the maximum desired velocity can move to the target.

3. Case Studies

To illustrate the practicalities of the proposed model, three different scenarios of pedestrian movement are simulated in this section.

3.1. Case 1: Uni-directional pedestrian traffic

A uni-directional pedestrian flow in a $12m \times 4m$ channel is simulated. The periodic boundary is used, where a pedestrian who exit from one side of the channel will entry from the other side of the channel. The simulation is of 10,000 time steps, and we take the last 5,000 time steps to get rid of the initial interference. In this case, the discretization effect on fundamental diagram and headway are studied.

3.1.1. Discretization

In many CA models in literatures, a pedestrian is assumed to occupy a $0.4m \times 0.4m$ square. For comparison with these literature results, in this case, a pedestrian is supposed to occupy $b=n^2$ grids. We take the maximum desired velocity to be $2m/s$. Then the space scale a is $0.4/n(m)$, and a time step is $0.2/n(s)$.

3.1.2. Definite conditions

(1) Boundary conditions

The static field of the position (x,y) is $S(x,y)=x \cdot n/0.4$.

Every time a pedestrian moves, the dynamic field of positions where the pedestrian leaves will

increases by 1, i.e., $D(t+1)=D(t)+1$. At the same time, the dynamic field decay with α and diffusion with β, i.e., $D(t+1)-D(t)=\alpha\cdot\Delta D(t)-\beta\cdot D(t)$. Here, $\alpha=0.05$ and $\beta=0.20$ to control the fluctuation.

K_S is 2.0, and K_D is 0 in this case.

(2) Initial conditions

The initial dynamic field in this case is set to be $D(x,y,t_0)=0$.

(3) Specific behaviors and characteristics

In this case, a pedestrian moves or steers. In every time step, a pedestrian steers with the constant transfer probability P_S, or moves with a desired velocity $\|v\| \quad N\left(1.34, 0.34^2\right)$. Then transfer probabilities governing movement and steering are determined. For example, if we take the maximum desired velocity to be $2m/s$, for a pedestrian with the current velocity $1.34m/s$, he has the probability of 67% to move to one of his neighbor grids (including the grid he currently occupies) in the next time step.

3.1.3. Results

- ***Discretization effect on fundamental diagram(FD)***

The fundamental diagram is the basic relation characterizing transport properties of pedestrian systems. Results of global/macroscopic measurement are presented (Jelić et al. 2012, Burghardt et al. 2013). The number of pedestrians N divided by the channel size A gives the global density ρ ($\rho=N/A$). The global average velocity is given by,

$$v=\frac{\sum_{i}^{N} v_i \times \cos\theta_i}{N} \tag{17}$$

where v_i is the actual velocity of pedestrian i, and θ_i is the angle between the moving direction and the longitudinal direction of the channel. According to the hydrodynamic relation, the global specific flow f is the multiple of the global density and the global velocity ($f=\rho\times v$).

The spatial discretization has an effect on the fundamental diagram in the high-density region with $\rho\geq 5.0m^{-2}$. For $n=1$ where a grid is occupied by exactly a pedestrian, the global velocity and specific flow is significantly higher, and the channel won't be completely jammed in high density region, as shown in fig.4. As long as a grid is empty, it can be occupied by a pedestrian in the next time step. But as for $n\geq 2$, the channel may reach a complete jam phase in the high-density region. That is because finer spatial discretization makes pedestrians range out of alignment, and because the hard-core exclusion principle that any possible overlaps of space in the walking direction of a pedestrian is forbidden makes that pedestrian has to stay.

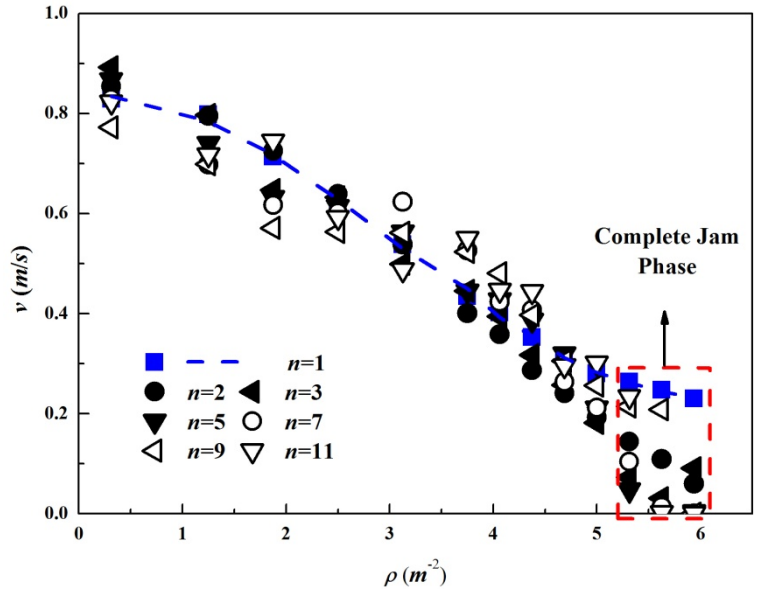

(a)

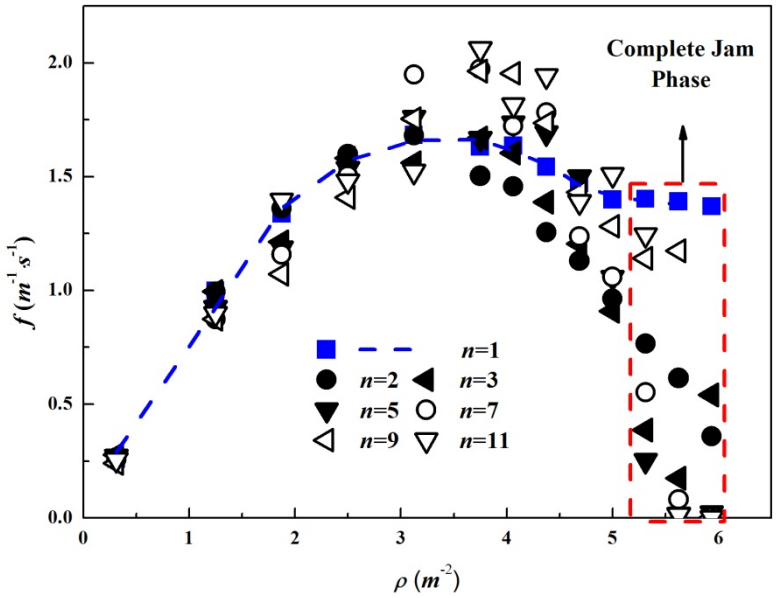

(b)

Fig.4. Significant discrepancy between FDs with n=1 and n≥2 (P_S=0.50).

- ***Discretization effect on Headway and Adaption Time***

The inter-person distance/headway h is measured between center coordinates of a pedestrian and its predecessor, and can be regarded as the required space needed for a pedestrian to walk at a certain velocity (Thompson and Marchant 1994). For a pedestrian flow of evenly space persons, the average headway h equals $\rho^{-0.5}$. Three linear regimes (Paris et al. 2007) with different slopes can be clearly distinguished, as shown in fig.5.:

(a) Free regime. Pedestrians tends to walk in their preferred velocity and do not seem to interact with each others.

(b) Intermediate regime/weakly constraint regime. The velocity depends on weakly on the inter-person distance, and pedestrians do not slow down to much.

(c) Jam regime/strongly constraint regime. The velocity is sharply decreased, and the jam becomes much more obviously as the headway goes down.

With the velocity approaching to zero, pedestrians remain at a certain minimal distance $h_0 \approx 0.4m$ which equals the thickness of a pedestrian from each other. The slope in each linear regime has the dimension of time, and can be interpreted as the sensitivity to the headway. It also can be described as an adaption time, as it is the time available to react before being at a minimal headway (the crossover of two neighbor regimes) from the current position of the predecessor in one regime (Jelić et al. 2012).

The characteristic adaption time does not vary smoothly but only takes three values with sharp transition between them. Table 1 summarizes the adaption time and the minimal headway of the three regimes. Regardless of the discretization effect, the adaption time and minimal headway in jam regime and intermediate regime remain relative stable values. Note that the simulation results of adaption time are much smaller than observations (Seyfried et al. 2005, Jelić et al. 2012). That is because pedestrians in observations are supposed to continue to move with lock-step when the headway reduces to be less than a thickness of a pedestrian. As the pedestrian density increases, the pedestrian's concentration on the movement reduces, resulting a reaction delay to its neighbors in front, and lock-step occurs. Pedestrian marching in lock-step and the optimization of the available space sufficiently enhances the traffic efficiency, especially in the special high density region.

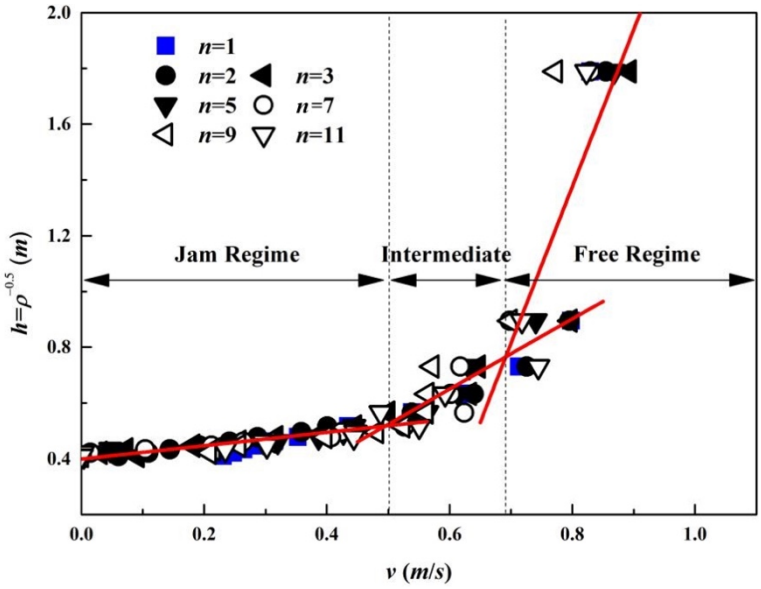

Fig.5. The headway $h=\rho^{-0.5}$ against the velocity v with different discretization factor n, and transitions from free to jam are observed.

Table 1. Adaption time and minimal distances of the three regimes measured in fig.5.

Phase	**Adaption time (*s*)**	**Minimal Headway(*m*)**	**R-Square**
Jam	0.24	0.40	0.81
Intermediate	1.26	0.52	0.75

Free flow	5.64	0.77	0.53

- ***Discretization effect on Computational Time***

The computational time is another thing one may concern. The simulation was run on a personal computer of an Intel Core i5-4590 CPU @ 3.30GHz and an 8.00GB RAM. The specific computational time of simulation t grows exponentially with the discretization factor n, as shown in fig.6. Compared with the discretization effect, the pedestrian density has little influence on the computational time. Thus, based on field surveys of simulation scenarios, we should balance the relationship between the structure accuracy and the computational efficiency.

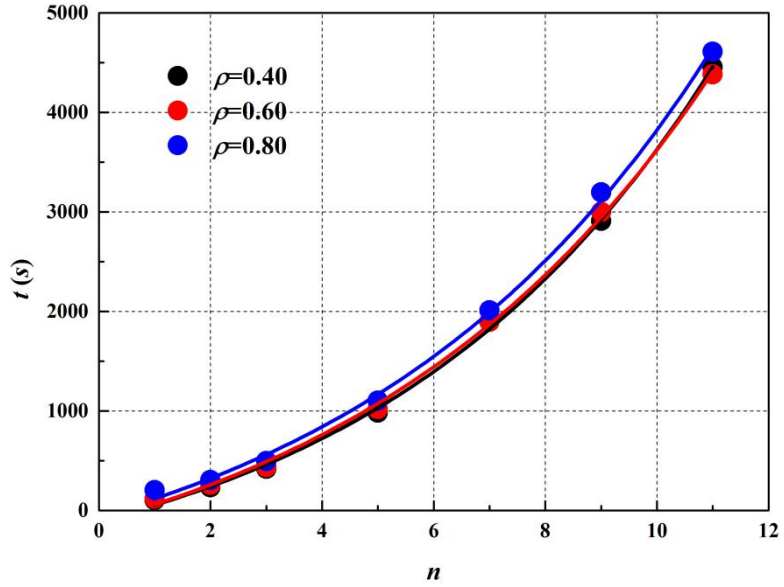

Fig.6. Computational time for 10,000 time step of simulation t against the discretization factor n

- ***Comparison with Empirical Data***

The simulation results are compared with the empirical data of Weidmann who gives one of the most elaborate fundamental diagram. In the simulation, according to Wirz et al. (2013), the desired velocity has a relationship with the current density as,

$$\left\| v(t) \right\| = 1.65 \times v_f \times \left\{ 1 - \exp\left[-1.913 \times \left(\frac{1}{\rho(t)} - \frac{1}{\rho_{\max}} \right) \right] \right\} \qquad (18)$$

where $\rho_{\max}$ is the observation maximum density, and equals $6.25m^{-2}$ (Weidmann 1992; Burstedde et al. 2001); v_f is the free velocity with a normal distribution $v_f \quad N\left(1.34, 0.34^2\right)$.

The simulation results fit well with the empirical data of Weidmann, as shown in fig.7. That indicates our model is reliable to catch the main features of the pedestrian flow.

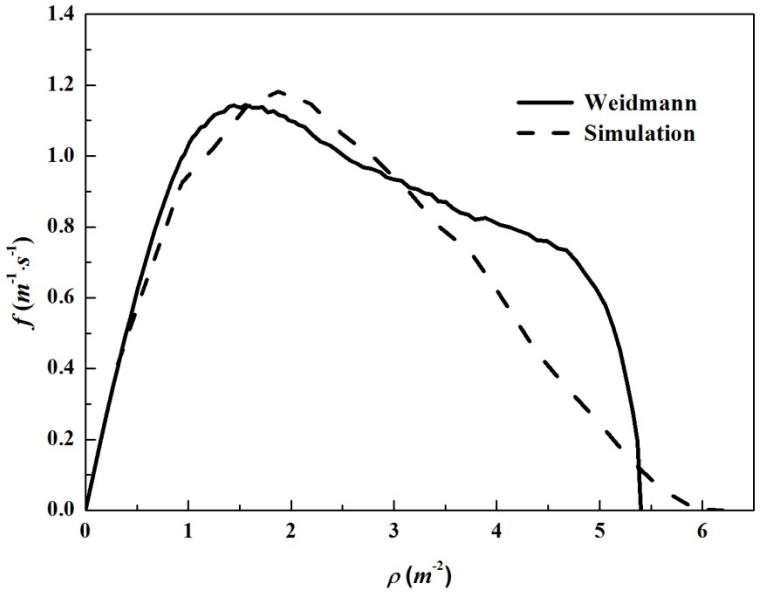

Fig.7. Fundamental diagram, comparing the simulation (dash) with the Weidmann (1992, solid).

3.2. Case 2: Pedestrian Evacuation from a Room

With initial random distribution, N=150 pedestrians are simulated to evacuate from an $8m \times 6m$ room where a $1.2m$ exit locates at the short wall. The initial average density is then $3.125per/m^{-2}$. 5 runs of simulation for each scenario were conducted.

3.2.1. Discretization

A pedestrian is supposed to occupy $b=n^2$ grids. We take the maximum desired velocity to be $2m/s$. Then the space scale a is $0.4/n(m)$, and a time step is $0.2/n(s)$.

3.2.2. Definite conditions

(1) Boundary conditions

The static field of the structure is calculated by the same method in Fu et al. (2013). The calculation method of dynamic field is the same as that of case 1. K_S is 2.0, and K_D is 0 in this case.

(2) Initial conditions

The initial dynamic field in this case is set to be $D(x,y,t_0)=0$.

(3) Specific behaviors and characteristics

In this case, a pedestrian moves or steers. In every time step, a pedestrian steers with the constant transfer probability P_S, or moves with a desired velocity $\|v\| \quad N\left(1.34, 0.34^2\right)$. Then transfer probabilities governing movement and steering are determined. The lateral movement speed is set to be half of forward movement speed, and the backward movement speed is set to be 1/3 of forward movement speed.

3.2.3. Results

Static fields with different discretizationl factor (n=1, n=11) are shown in fig.8., where we can

find that the finer spatial discretization leads to a better approximation of the continuous field and more accurate representation of the geometric structure.

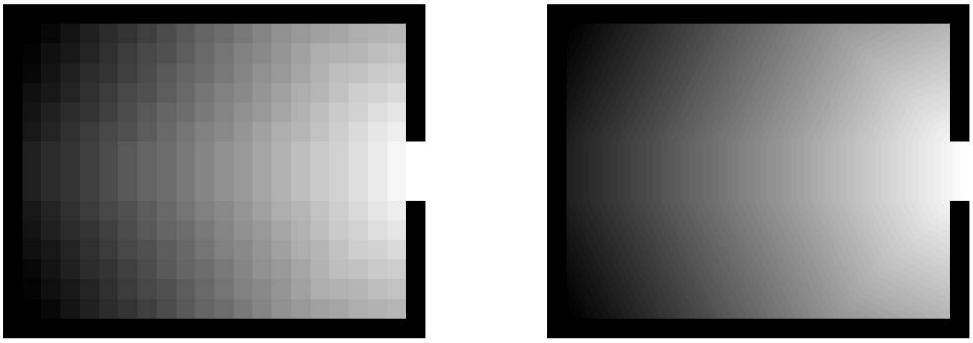

(a) (b)

Fig. 8. Comparison of static field of a $8m\times6m$ room with the length scale (a) a=0.4m, n=1, where the model degenerates to the traditional cellular automaton, and (b) $a\approx3.6\times10^{-2}m$, n=11

- ***Evacuation time***

Parameters related to time are illustrated as following,

Name	Meaning	Unit
t^*	The evacuation duration measured by the unit of time step	*time step*
T	$T=t^*\times\Delta t$, the evacuation duration measured by the unit of second	*second*
t	The computational time spent for simulation	*second*
τ^*	$\tau^*=t/t^*$, the computational time spent for each time step of the simulation, i.e., response time	*s/time step*
τ	A dimensionless computational time, which is spent for each second of the simulation, i.e., the proportion of the computational time to the time duration in simulation ($\tau=t/T$)	*1*

The total evacuation time (*TET*) from the beginning of evacuation to the time when the last pedestrian evacuate from the room and the average evacuation time (*AET*) are the main two time indicators to evaluate evacuation efficiency. *AET* equals the sum of individual evacuation times dividing the number of pedestrians. Fig.9. gives the *TET*, *AET* against the discretization factor n and *transfer probability* for steering P_S. Because of queuing at the bottleneck/exit, the *TET* is significantly higher than *AET*. The *TET* is usually nearly twice of the *AET*. Since pedestrians have different walking abilities (the pedestrian free velocity is Gaussian distributed), *TET* fluctuates in a small range with the discretization factor n. The *TET* is always determined by the slowest pedestrians who also have a disadvantage in the competition. *AET*, which reflects the overall average evacuation efficiency, is more stable. A sudden change of *AET* occurs between n=1 and n=2. Because finer discretization may lead to additional blockage near bottlenecks (Kirchner et al. 2004), the *AET* for n=1 is 11.9% smaller than those for $n\geq2$. Such additional blockage phenomenon will not appear in coarse discrete models, for example, in traditional CA models. As shown in fig.10(a) below, with n=1, the whole exit can be used efficiently. The exit can be occupied by three pedestrians at the same time step. As shown in fig.10(b), the space is finer

discretized with n=2. Pedestrians in shadow positions are blocked, and they can not walk through the exit. With the usage of the exit decreasing, and the average evacuation time increases.

Quite different from results of previous works (Guo 2014, Xu et al. 2008, Weng et al. 2007), the evacuation time is independent on the spatial discretization as it should be. In previous works, to realize a maximum velocity v_{max}>1, pedestrians are supposed to move multiple cells per time step in straight resulting unrealistic trajectories of pedestrians. Thus, with n=v_{max}, agents in simulation are aligned in rows, and under that condition both *TET* and *AET* are smallest. By introducing the *transfer probability* for moving/staying mentioned in eq.(7), the unrealistic trajectories and alignment of pedestrians are avoided.

The *transfer probability* for steering P_S has little influence on both the *TET* and the *AET*. That is because, in a few time steps of simulation, most of the evacuating pedestrians steer to the direction with the maximum potential field λ_{max}. *TET* fluctuates in a small range, because of different walking abilities of pedestrians and dominant effect of these slowest pedestrians. The *AET* is more stable. In the following section, we will further discuss how long it takes that pedestrians steer to the maximum potential field.

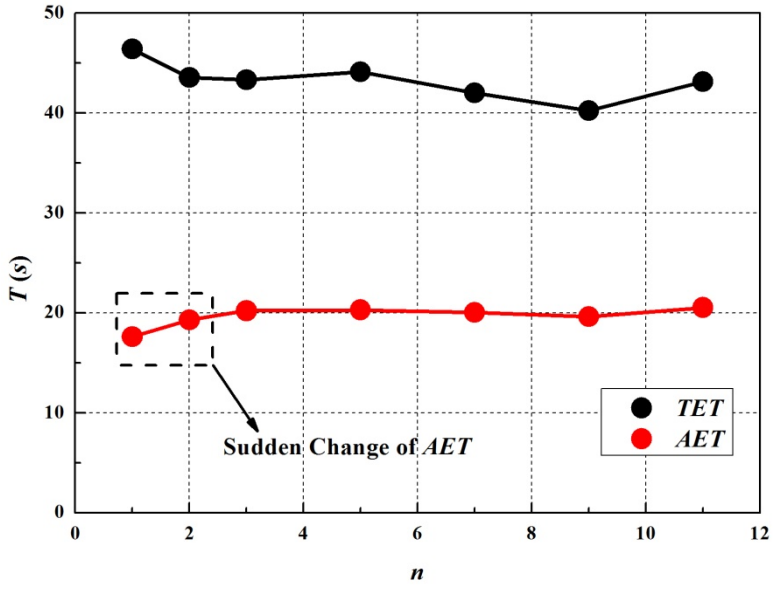

(a)

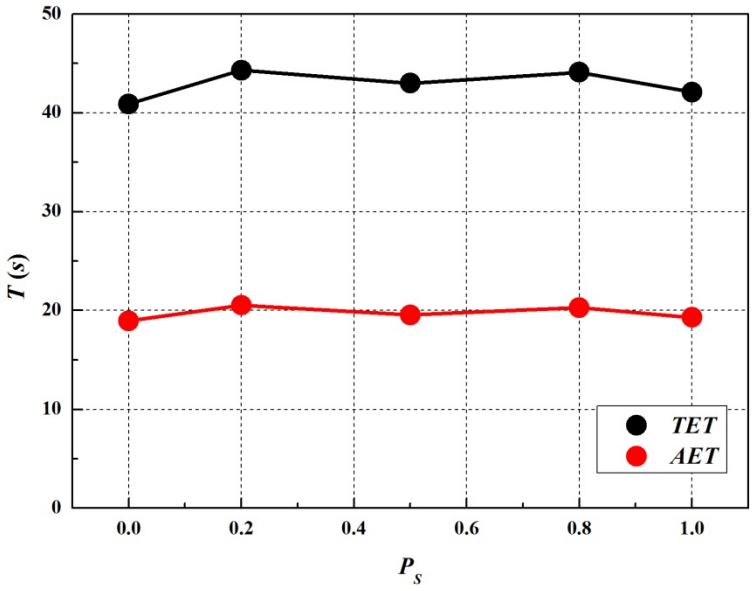

(b)

Fig. 9. Total evacuation time(*TET*) and average evacuation time(*AET*) against (a) the discretization factor n with P_S =0.5, and (b) steering probability P_S with n=3

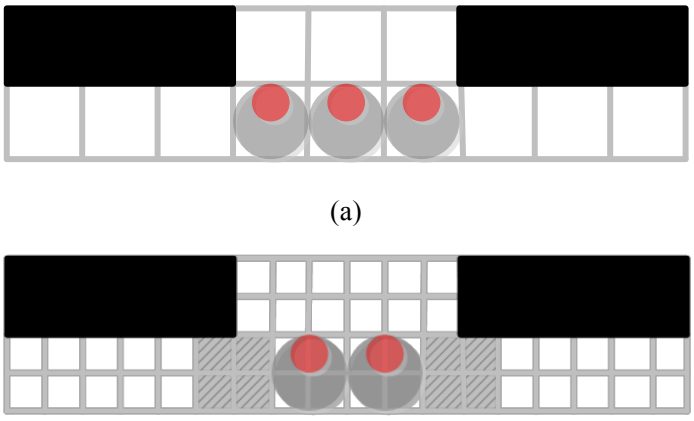

(a)

(b)

Fig.10. Pedestrians at the bottleneck with the door width 1.2*m*. (a)With the spatial scale a=0.4*m* (n=1), the exit is used efficiently. (b) Additional blockage appears with the sptial scale a=0.2*m* (n=2)

- ***Conflicts***

The conflict number (C_n) is the number of pedestrians involving in conflicts during a second. The conflict frequency (C_f) is defined as the average frequency of pedestrians involving conflicts during a second, and can be given by,

$$C_f = \frac{\int \frac{C_n(t)}{N_R(t)} \mathrm{d}t}{\int \mathrm{d}t} \tag{19}$$

where N_R is the number of residual pedestrians in the system.

Even though spatial discretization has little influence on pedestrian evacuation time, the conflict

frequency increase almost linearly with the discretization factor n under the condition of $n \geq 2$. It is interesting to observe that the average conflict frequency ($\bar{C}_f$, unit: $per^{-1} \cdot s^{-1}$) of evacuation plateaus where the conflict frequency remains relative constant (Kirchner, 2003) has a linear relationship with the discretization factor n, as shown in fig.11., which can be formulated as,

$$\bar{C}_f = 7.79 \times 10^{-2} n + 1.75 \times 10^{-1} \left(R^2 = 0.996 \right) \text{ for } n \geq 2. \tag{20}$$

One of the possible reason for this linear relationship is that the out of alignment of pedestrians, whose probability is proportional to the discretization factor n, increases the conflict frequency, since overlapping of any part of pedestrian body is forbidden due to the exclusion principle.

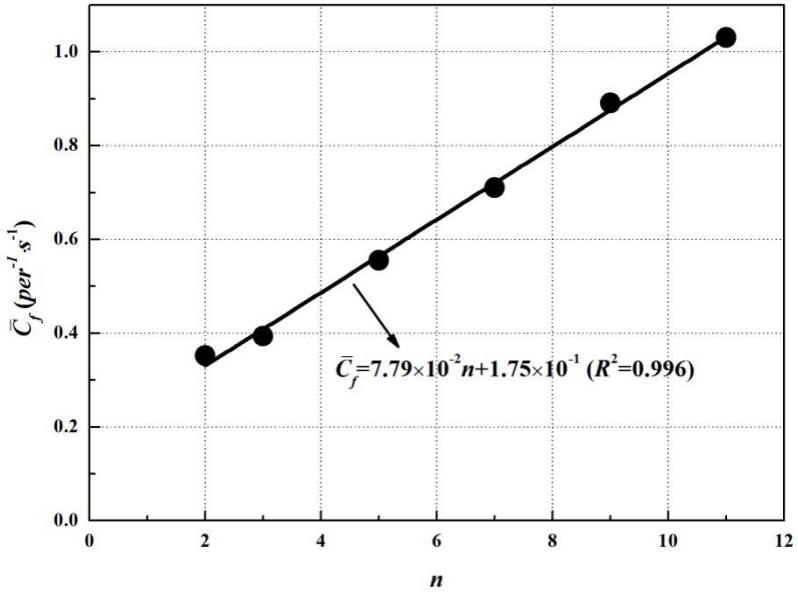

Fig. 11. Average conflict frequency of evacuation plateaus has a relationship with the discretization factor n(P_S=0.5)

In very few seconds, most pedestrians steer to the direction with the highest potential field $\lambda_{\max}$, as shown in fig.12. The order parameter is calculated by,

$$O = \frac{\left| \sum_{i=1}^{N_R} \lambda_i \right|}{N_R} \tag{21}$$

where λ_i is the unit vector of the moving direction for pedestrian i, and $0 \leq O \leq 1$. If all pedestrians walk randomly, O equals 0. Otherwise, if all pedestrians move in the same direction, O equals 1.

Pedestrians tend to move along paths in the normal direction of potential field, and thus pedestrians flow out from the exit orderly.

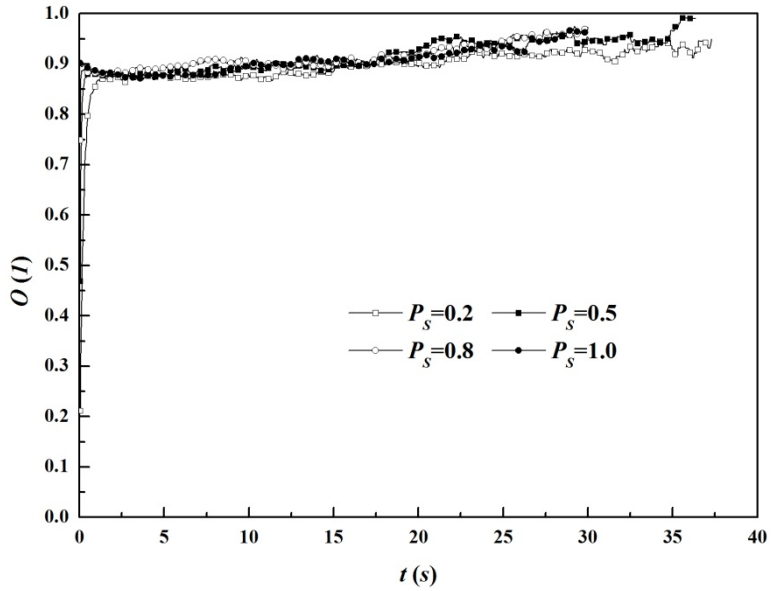

Fig.12. Order parameter evolution under different *transfer probability* to steer (n=3)

- ***Computational time***

The simulation was run on a personal computer of an Intel Core i5-4590 CPU @ 3.30GHz and an 8.00GB RAM. Running on other computers with different computer configurations, the computational time might be different, but the trends of these *t*-*n* curves are believed to be similar. As long as n is larger than 10, further increase of n-value has little influence on the changes of geometric scale. But as shown in fig.13., the computational time spent for the whole evacuation process t, the computational time spent for every second of evacuation τ, and the response time τ^* (computational time spent for a time step) increase exponentially with the discretization factor n, and can be formulated as,

$$t = 55.5\mathrm{e}^{0.312n} - 86.7 \ \left(R^2 = 0.999\right) \tag{22}$$

$$\tau = 1.63\mathrm{e}^{0.293n} - 2.65 \ \left(R^2 = 0.997\right) \tag{23}$$

$$\tau^* = 0.088\mathrm{e}^{0.168n} - 0.1 \ \left(R^2 = 0.997\right) \tag{24}$$

Thus, based on surveys of a specific scenario, we have to balance the relationship between the accuracy and the computational efficiency. Time steps spent for evacuation t^* increases linearly with the discretization factor n, and a time step grows in inverse proportion to the discretization factor n. So the *TET* and the *AET* remain independent with n-value.

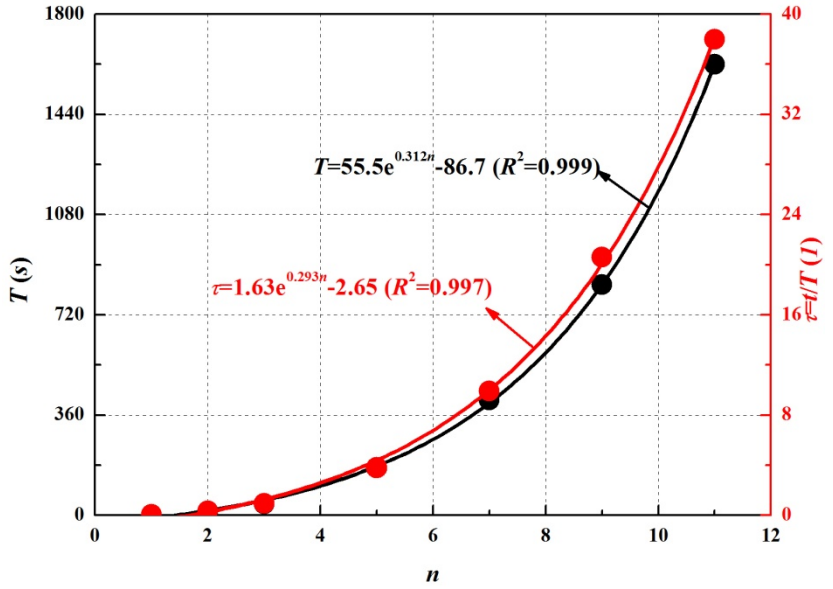

(a)

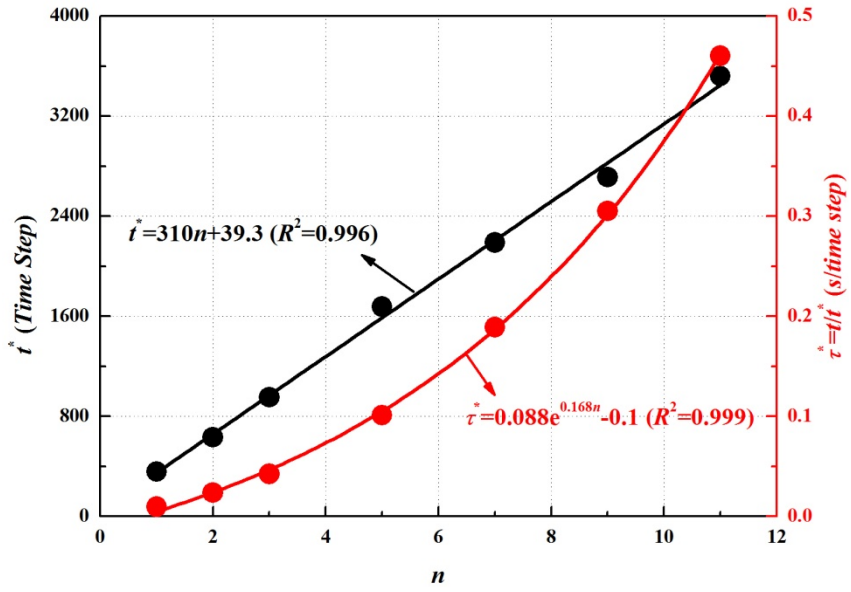

(b)

Fig.13. (a) computational time for the whole evacuation process t and computational time for every second of evacuation τ, (b) time steps t^* spent for evacuation and response time τ^* against the discretization factor n

The computation time t of the model against the number of individuals N is shown in fig.14. When the number of individuals is less than 500, the evacuation distance is the dominant factor that determines the evacuation time and the computation time. Under this condition, pedestrians have to travel a long distance before they reach the exit, and the computation time remains almost unchanged. When the number of individuals is greater than 500, the bottleneck effect of the exit becomes dominant. Pedestrians have to queue, and the arch around the exit appears. The evacuation time and the computation time increase. As the number increases to 10,000, it takes about 13 hours to run the simulation. But for an evacuation of 1,000 individuals, it only takes 3.35 minutes to rum the simulation. (In this scenario, pedestrians evacuate from a $40m \times 40m$ room with

a 2*m* door in the middle of one wall. Pedestrians initially distribute randomly. All pedestrians have the same 1.34*m*/*s* desired velocity. The maximum number of evacuation pedestrians is 10,000. The discretization factor *n* takes 1.)

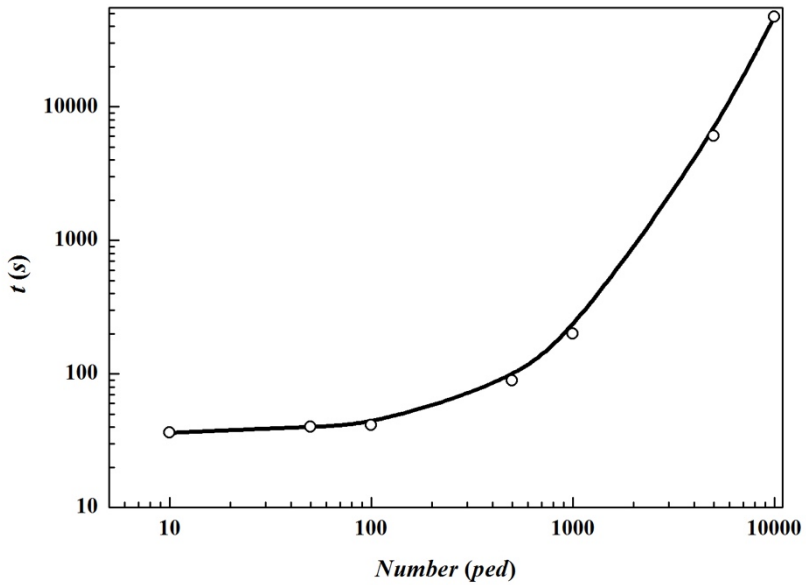

Fig.14. The computation time *t* against the number of evacuation individuals

- ***Comparison with Experiment Data***

The simulation results are compared with the experiment data (Nagai et al. 2006; Kretz et al. 2006; Müller, 1981) in terms of the flow at the bottleneck/exit. Under these scenarios, pedestrians walk through a 1.2*m* door. As shown in fig.15, the simulation results are close to Nagai's experiment data and within the range of the Müller's.

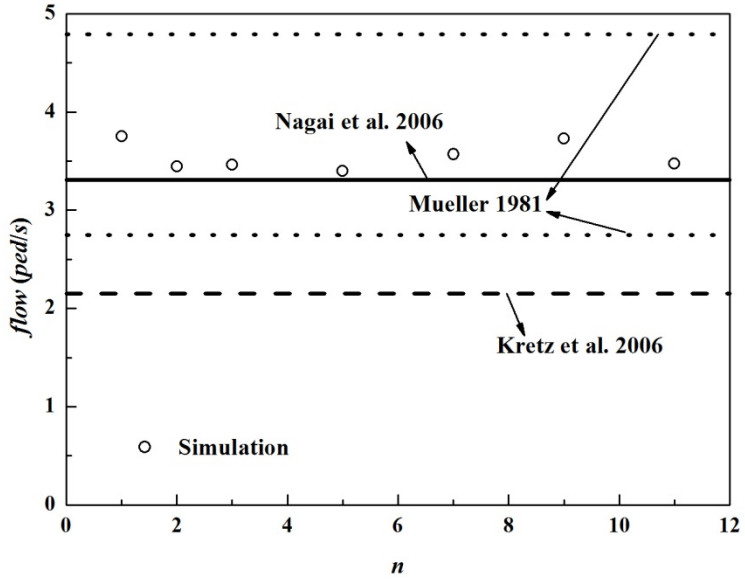

Fig.15. Flow at the bottleneck under different discretization factors *n*, comparing the simulation (circles) with the experiment data (lines, Nagai et al. 2006; Kretz et al. 2006; Müller, 1981).

3.3. Case 3: Ascending Evacuation in a 21-Storey Stair

We conduct a long ascent evacuation simulation in a 21-storey stair. The structure of the stair system and the detail of the stair connecting the 12th floor and 11th floor (circled in fig.16.(a)) are shown in fig.16. Each entrance and exit has the same width of 1.2*m*. 50 pedestrians initially distribute in the system randomly, and 1,000 pedestrians entry the 21-stoery stair system from each entrance (blue lines in fig.16(a) and 16(b)) with the inflow 1.5*ped*/(*m*·*s*). Each exit links the flight of its neighbor stair, and there is a terminal exit located on the top floor (the right bottom corner), towards which the pedestrians move. Pedestrians move with fatigue or with constant speed (comparable group) in this case.

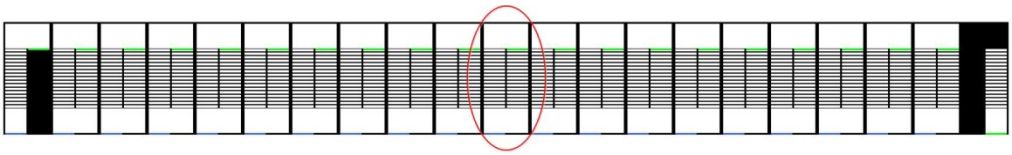

(a)

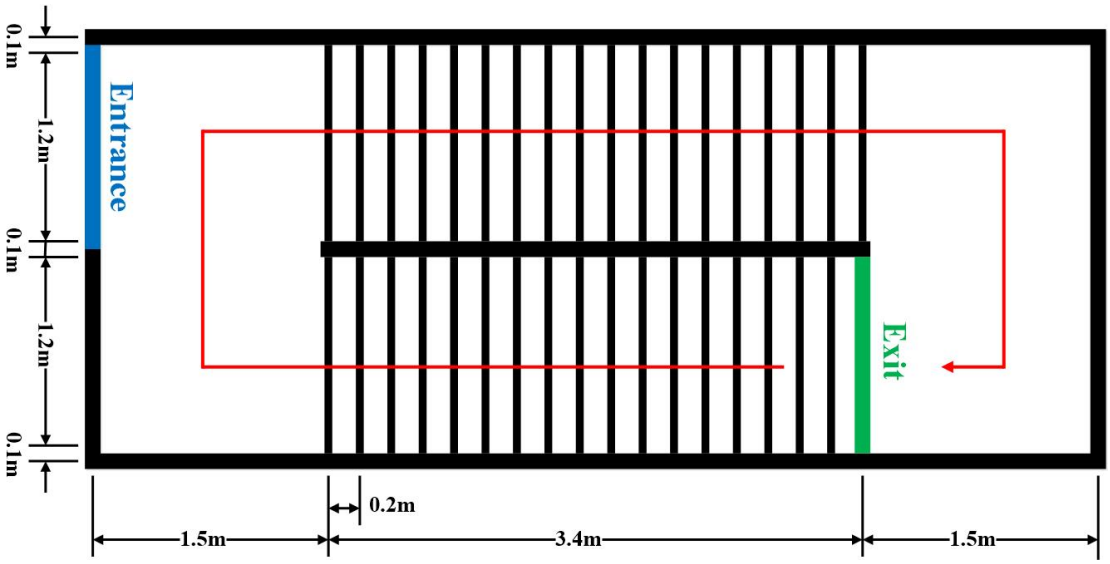

(b)

Fig.16. (a) the structure of the stair system, and (b) the detail of the stair connecting the 12th floor and 11th floor underground

3.3.1. Discretization

The step depth of stairs in apartments is suggested to be 0.26*m*-0.30*m* (National Standard of People's Republic of China, GB50096-2011, 2011), which is almost half of a pedestrian width. One can find another example in Liu et al. (2014b). In the economy class of a commercial civil aircraft, the width of legroom is around 0.3*m*, whereas the seat is around 0.5*m*. Additionally, according to the statistics of human dimensions of Chinese adults (National Standard of People's Republic of China, GB-10000-88, 1988), the width of an adult is almost twice of the depth. So a pedestrian is supposed to occupy $b=n^2/2$ grids. $n=4$ is used in this case. A pedestrian configuration is shown in fig.17. We take the maximum desired velocity to be 2*m*/*s*. Then the space scale a is 0.1*m*, and a time step is 0.05*s*.

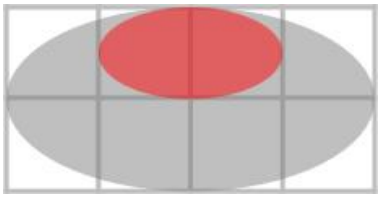

Fig.17. the configuration of a pedestrian in simulation of evacuation in a 21-storey stair

3.3.2. Definite Conditions

(1) Boundary conditions

To calculated the static field, we considered the attract of exits and the repulsion of obstacles, in this case, walls and handrails. The static field generated by exits S_E is calculated as the same as Fu et al.(2013), and the static field generated by obstacles S_o is calculated as following,

Step 1.	Set $S_o(i,j)=0$, $\sigma(i,j)=1$ for each grid of obstacles (walls and handrails). Set $S_o(i,j)=0$, $\sigma(i,j)=0$ for other grids of structure.
Step 2.1.	For the Neumann neighbor cell (i,j) of the cell (i_0,j_0), set $S_o(i,j)=S_o(i_0,j_0)+1$, if $S_o(i,j)=0$, $\sigma(i,j)=0$.
Step 2.2.	End if all grids of structure $\sigma(i,j)=1$, else go back to **Step 2.1**.

Then, the static field of the whole structure is set to be $S=S_E+0.5\times S_o$.

Every time a pedestrian moves, the dynamic field of positions where the pedestrian leaves will increases by 1, i.e., $D(t+1)=D(t)+1$. At the same time, the dynamic field decay with α and diffusion with β, i.e., $D(t+1)-D(t)=\alpha\cdot\Delta D(t)-\beta\cdot D(t)$. Here, $\alpha=0.05$ and $\beta=0.20$ to control the fluctuation. The two sensitivity parameters of static field and dynamic field K_S and K_D is set to be 0.8 and 0.1.

(2) Initial conditions

The initial dynamic field in this case is set to be $D(x,y,t_0)=0$.

(3) Specific behaviors and characteristics

Since long-distance climbing stairs is simulated, fatigue is unavoidable. From previous study (Chen 2017), we know that the desired velocity for a pedestrian has a relationship with the distance which can be denoted as,

$$\|v\| = \begin{cases} 1.29 - 8.63\times10^{-3}\times d & d \le 69.45 \\ 0.69 & d > 69.45 \end{cases} \tag{25}$$

where d is the distance that a pedestrian have walked.

In the comparable group, pedestrians moves along their whole paths with a constant desired velocity 1.34m/s.

The rotation speed we assume is $2\pi s^{-1}$, and pedestrians are supposed to steer on only platforms.

As the definite conditions are determined, transfer probabilities regarding directions, moving or staying, and steering can then be calculated by eqns.(5), (7), (9), (10).

3.3.3. Results

- Evacuation Evolution with/without Fatigue

Snapshots of evacuation in the stair system under the situations that pedestrian moves with

constant speed and moves with fatigue can be found in fig.18. and fig.19. respectively. At the beginning of evacuation, the pedestrian distributions under the two situations are almost the same. But as the time goes by, the fatigue comes to be a dominant factor effecting the evacuation efficiency. An interesting phenomenon that even though there are jams in the middle parts of the stair system, pedestrians moves almost freely in the last part of stairs (the rightmost stair) is observed.

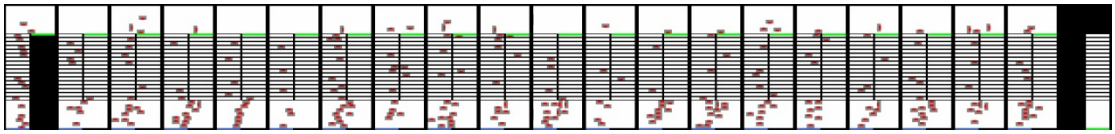

(a) 10*s*

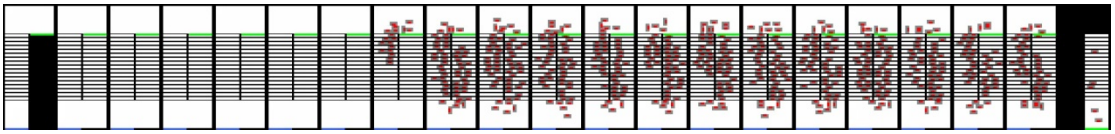

(b) 600*s*

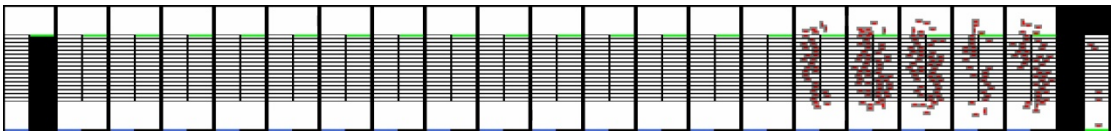

(c) 1200*s*

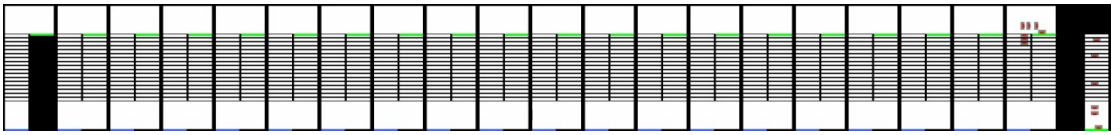

(d) 1500*s*

Fig.18. Snapshots of pedestrian distribution in the stair system without considering fatigue (comparable group) at (a)10*s*, (b)600*s*, (c)1200*s*, and (d)1500*s*

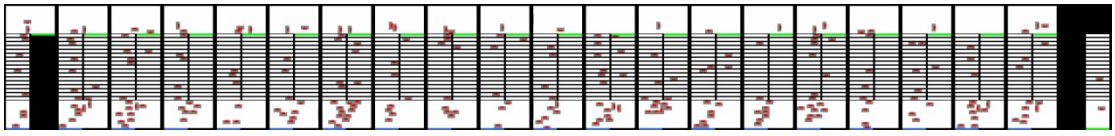

(a) 10*s*

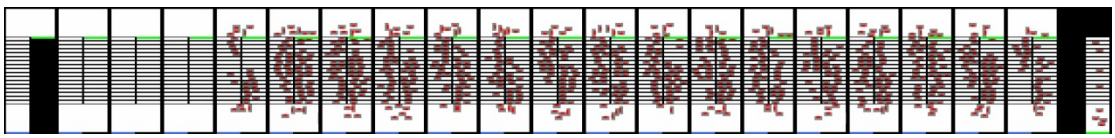

(b) 600*s*

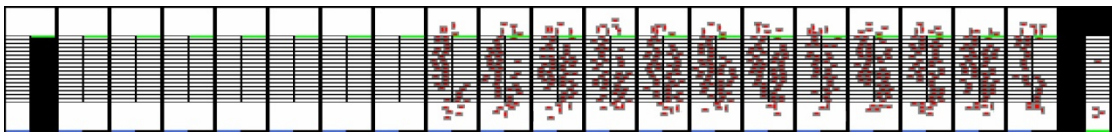

(c) 1200s

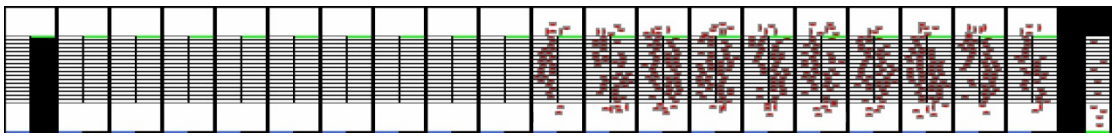

(d) 1500s

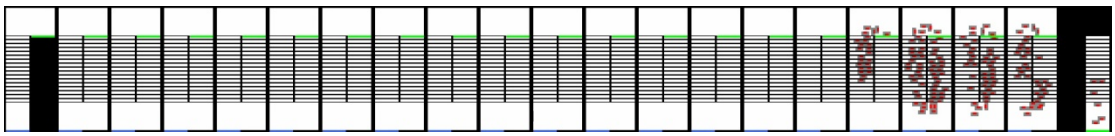

(e) 2400s

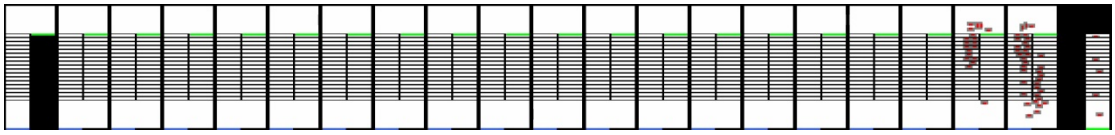

(f) 2700s

Fig.19. Snapshots of pedestrian distribution in the stair system considering fatigue at (a)10*s*, (b)600*s*, (c)1200*s*, (d)1500*s*, (e)2400*s*, and (f)2700*s*

The inflow and outflow of the stair system under the situations of constant speed and fatigue can be observed in fig.20. For both situations, 1,000 pedestrians move into the system in a short time(about 62*s*). The evacuation time(2857*s*) of 1,050 pedestrians under the situation of fatigue is almost twice of that under the situation of constant speed(1516*s*). The outflow for the situation of constant speed and fatigue is 0.83*ped*/(*m*·*s*) and 0.31*ped*/(*m*·*s*).

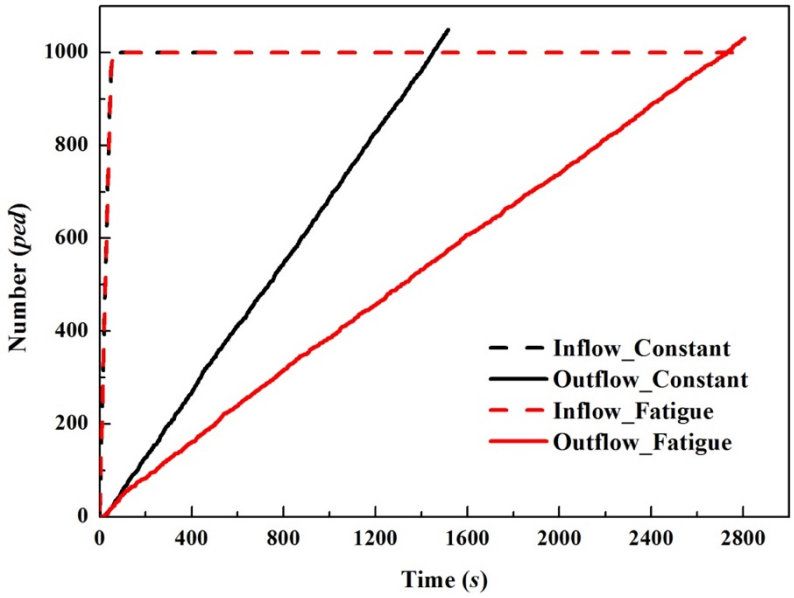

Fig.20. Inflow(dash) and outflow(solid) of the stair system under the situations of constant speed(dark) and fatigue(red)

- Comparison with Experiment Data

The '*Time-Cumulative Evacuation Number*' curve of the simulation is compared with the curve of experiment (Chen et al. 2018. The authors have got the authority to access the experiment data).

The experiment was conducted in a 26-storey residential building in Chengdu. 161 college students took part in this experiment, and they were randomly allocated into 4 groups. They were told to evacuate as quick as possible in advance as if the building had been got fire. The four groups participants were pre-distributed to the 1st, 2nd, 3rd, and 4th floors at the begin of the experiment. The participants on the 1st floor started to evacuate first. When the fastest person arrived at the 2nd floor, the participants on the 2nd floor started their evacuation. In similar fashion, participants on the 3rd and 4th floors started to evacuate only once the first walker reached their floor. The distance of 16 floors in the experiment is equal to the distance of 8 floors in our simulation. In the revised manuscript, we compared our simulation results (evacuation from the 1st floor to the 9th floor) with the experimental data (evacuation from the 4th floor to the 20th floor). Overall, the simulation results fit well with experiment data (See fig.21. below). The maximum difference between the simulation and the experiment appears at N=145. When the cumulative evacuation number N reaches 145, the evacuation time of experiment is 404s, while the evacuation time of simulation is 479s. The difference results from situations in which pedestrians are. In the experiment pedestrians were told to evacuate as soon as possible, while in the simulation of the case 'Ascending evacuation from a 21-storey stair' pedestrians walk under normal condition. The desired velocity under normal condition is bit lower than that under emergency evacuation condition.

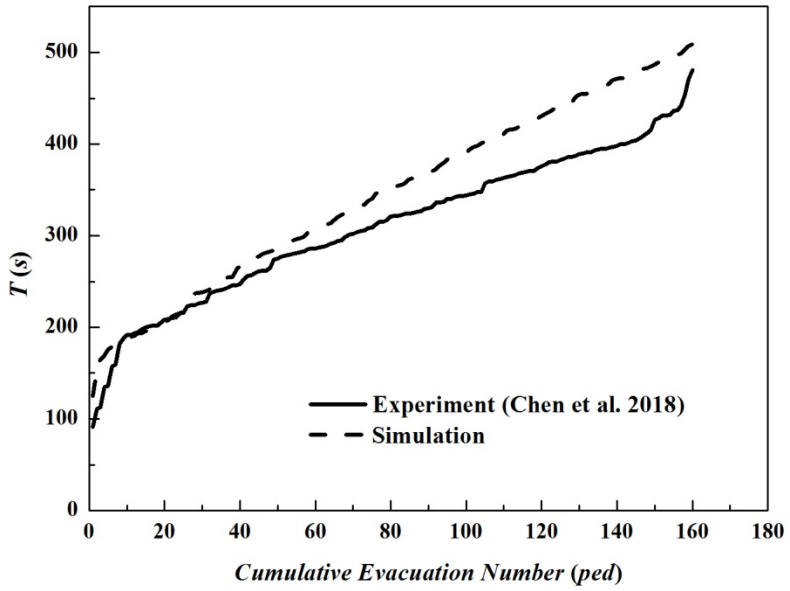

Fig.21. The evacuation time against the number of pedestrians evacuating from the 4th floor to the 20th floor, comparing the simulation (dash) with the experiment data (solid, Chen et al. 2018).

4. Discussion

(1) By only adjusting definite conditions, the proposed model has been used in three different cases, including both some simple typical systems like uni-directional flow (case 1) and evacuation from a room (case 2) and the complex stair system considering fatigue (case 3) and. In another paper, we also use this model simulate pedestrian movement in a quite complex building considering visual fields. All these indicates that the proposed model has a good flexibility and extendibility.

(2) As shown in fig.8., with the finer spatial discretization, the constructed field tend to be a approximation of the continuous field and a more accurate the geometric structure is represented. Pedestrian alignment is avoided, and the evacuation time no longer has a relationship with the discretization factor. Regarding trajectories of pedestrians, the finer space discretization yields more accurate approximation of the actual trajectories in the following ways

- Details of pedestrian trajectories (e.g. turning) can be well caught as shown in fig.22;
- The travelled distance is closer to the actual distance seen in fig.17;
- Both the maximum deviation and the average deviation from the actual trajectory become smaller.

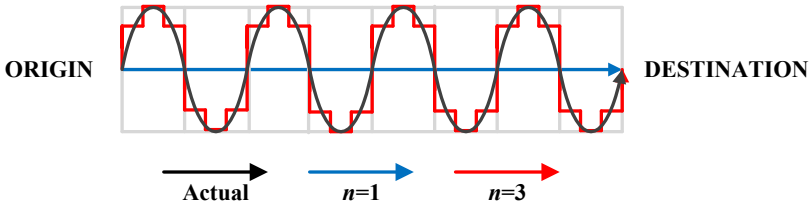

Fig. 22. Expected trajectories of pedestrians with n=1 and n=3 compared with the actual trajectory. Manhattan distance from the origin to the destination is used.

As shown in fig.23, trajectories of 50 pedestrians evacuating from the 21st floor underground to the ground floor is are consistent with these observations (Hoskins and Milke, 2012; Chen et al. 2017): 1) the trajectories on the platforms are semi-circles whose average radius is nearly half of the stair width; 2) on average, pedestrians tend to walk along the central line of the stairs when they climb.

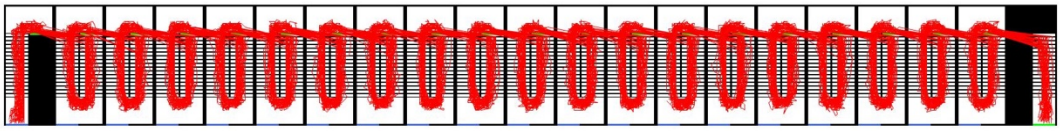

Fig. 23. Trajectories of 50 pedestrians in the 21-storey stair system by the proposed model

Our simulation results fit well with empirical/experimental data (See fig.7, fig.15, and fig.21).

(3) Not only is the transfer probability of traditional floor field CA model determining moving direction included in the proposed model, but also we bring new ideas of transfer equations/probabilities determining moving/staying and steering. By these transfer equations, different walking abilities including different walking speed and turning speed of pedestrians (heterogeneity), direction-dependant characteristics (anisotropy, for example, side stepping), and time-dependant characteristics (for example, fatigue and visual field) can be easily realized.

(4) For a speed increment of 0.1m/s, comparing with previous finer discrete models (e.g. Kirchner et al. 2004) which need to use at least 10 time steps to realize a movement of a speed larger than 1m/s, our model only requires 1 time step. For previous models with fine spatial discretization, if the pedestrian reaches a speed greater than 1m/s, a time step in existing models has to be divided into several sub-steps, and conflicts should be resolved in each sub-step, which is quite complex and time consuming. In contrast, such division of one time step is no longer needed in our model. But we should also note that the computational time consumed increase exponentially with the discretization factor. Thus, based on surveys of a specific scenario, we have to balance the relationship between the accuracy and the computational efficiency.

5. Summary

In order to simulate the pedestrian traffic in a more accurate, extendable and less computational consuming way, a discrete field model was proposed integrating the heterogeneity, anisotropy, and time-dependant characteristics of pedestrian traffic. The heterogeneity of pedestrian traffic means that properties of a individual differ from properties of other individuals. The anisotropy is that each pedestrian has different walking properties in different directions, and time-dependant characteristic is that properties of the pedestrian change along the path.

In the proposed model, pedestrians which are modeled as independent-thinking agents are driven by *transfer equations* governing movement direction, moving/staying and steering. By combining *transfer equations* and *definite conditions*, *transfer probabilities* are obtained. Comparing with previous researches on finer discrete CA models, the proposed model has advantages in flexibility, higher accuracy spatial scale, wider speed range, relative low computational cost, and elaborated conflict resolution with synchronous update scheme.

In the three specific scenarios, the simulation results fit well with empirical/experiment data.

(1) In the case of unidirectional pedestrian flow in a channel, by the proposed finer discrete model, one can observe a complete jam where the average velocity approaches to zero in high density region. This complete jam can not be observed in the simulation by traditional floor field CA models, since pedestrians always align with each other. Three linear regimes, namely free regime, intermediate regime and jam regime, are observed along the entire distance of the relationship between the headway and the velocity. The space discretization have little influence on the adaption time and the minimal headway of the jam phase and the intermediate phase.

(2) In the case of evacuation from a room, because unrealistic pedestrian trajectory (see fig.22.) is partially avoided by finer time step and *transfer equation* governing moving/staying, and unrealistic alignments of pedestrians are then avoided. Thus, both the total evacuation time and the average evacuation time are independent on the discretization factor as it should be, which is quite different from previous works. It is also interesting to observe that the average conflict frequency has a very good linear relationship with the discretization factor. In few seconds, the order parameter reaches to a steady value. Pedestrians tend to rotate to and move along paths in the normal direction of the potential field, and pedestrians walk out of the room orderly.

(3) In the case of long ascending evacuation in a 21-storey stair system, that pedestrians move with constant speed or with fatigue is simulated. The evacuation time(2857*s*) of 1,050 pedestrians under the situation of fatigue is almost twice of that under the situation of constant speed(1516*s*). An interesting phenomenon that even though there are jams in the middle parts of the stair system, pedestrians moves almost freely in the last part of stairs(the rightmost stair) is observed.

Acknowledge

This research was supported by National Natural Science Foundation of China (No.11602206, and No.71573215). We especially thank Jianyu Wang for his supply of the experiment data.

References

Burghardt, S., Seyfried, A., & Klingsch, W. (2013). Performance of stairs–fundamental diagram and topographical measurements. *Transportation research part C: emerging technologies*, *37*, 268-278.

Burstedde, C., Klauck, K., Schadschneider, A., & Zittartz, J. (2001). Simulation of pedestrian dynamics using a two-dimensional cellular automaton. *Physica A: Statistical Mechanics and its Applications*, *295*(3), 507-525.

Chen, J., Wang, J., Wang, J., Liu, X., Li, T., & Lin, P. (2017). An experimental study of individual ascent speed on long stair. *Fire Technology*, *53*(1), 283-300.

Chen, J., Hao, Y., Wang, J., Wang, P., Liu, X., Lin, P. (2018). An experimental study of ascent and descent: movement of people on long stairwells with high occupant density. *Fire Technology*, (under the 2nd round review)

Fu, Z., Yang, L., Chen, Y., Zhu, K., & Zhu, S. (2013). The effect of individual tendency on crowd evacuation efficiency under inhomogeneous exit attraction using a static field modified FFCA model. *Physica A: Statistical Mechanics and its Applications*, *392*(23), 6090-6099.

Fu, Z., Zhou, X., Chen, Y., Gong, J., Peng, F., Yan, Z., Zhang, T., Yang, L. (2015a). The influence of random slowdown process and lock-step effect on the fundamental diagram of the nonlinear pedestrian dynamics: An estimating-correction cellular automaton. *Communications in Nonlinear Science and Numerical Simulation*, *20*(3), 832-845.

Fu, Z., Zhou, X., Zhu, K., Chen, Y., Zhuang, Y., Hu, Y., Yang L., Chen C., Li, J. (2015b). A floor field cellular automaton for crowd evacuation considering different walking abilities. *Physica A: Statistical Mechanics and its Applications*, *420*, 294-303.

Fu, Z., Luo, L., Yang, Y., Zhuang, Y., Zhang, P., Yang, L., Yang H., Ma J., Zhu K., Li, Y. (2016). Effect of speed matching on fundamental diagram of pedestrian flow. *Physica A: Statistical Mechanics and its Applications*, *458*, 31-42.

Guo, R. Y., & Huang, H. J. (2008). A modified floor field cellular automata model for pedestrian evacuation simulation. *Journal of Physics A: Mathematical and Theoretical*, *41*(38), 385104.

Guo, R. Y., Huang, H. J., Wong, S. C. (2012). Route choice in pedestrian evacuation under conditions of good and zero visibility: Experimental and simulation results. *Transportation research part B: methodological*, *46*(6), 669-686.

Guo, R. Y. (2014). New insights into discretization effects in cellular automata models for pedestrian evacuation. *Physica A: Statistical Mechanics and its Applications*, *400*, 1-11.

Helbing, D., Molnár, P., Farkas, I. J., Bolay, K. (2001). Self-organizing pedestrian movement. *Environment and planning B: planning and design*, *28*(3), 361-383.

Helbing, D., Buzna, L., Johansson, A., & Werner, T. (2005). Self-organized pedestrian crowd dynamics: Experiments, simulations, and design solutions. *Transportation science*, *39*(1), 1-24.

Hoskins, B. L., & Milke, J. A. (2012). Differences in measurement methods for travel distance and area for estimates of occupant speed on stairs. *Fire Safety Journal*, *48*, 49-57.

Hughes, R. L. (2002). A continuum theory for the flow of pedestrians. *Transportation Research Part B: Methodological*, *36*(6), 507-535.

Jelić, A., Appert-Rolland, C., Lemercier, S., & Pettré, J. (2012). Properties of pedestrians walking in line: Fundamental diagrams. *Physical Review E*, *85*(3), 036111.

Kirchner, A., Nishinari, K., & Schadschneider, A. (2003). Friction effects and clogging in a cellular automaton model for pedestrian dynamics. *Physical review E*, *67*(5), 056122.

Kirchner, A., Klüpfel, H., Nishinari, K., Schadschneider, A., & Schreckenberg, M. (2004). Discretization effects and the influence of walking speed in cellular automata models for pedestrian dynamics. *Journal of Statistical Mechanics: Theory and Experiment*, *2004*(10), P10011.

Kretz, T., Grünebohm, A., & Schreckenberg, M. (2006). Experimental study of pedestrian flow through a bottleneck. *Journal of Statistical Mechanics: Theory and Experiment*, *2006*(10), P10014.

Liu, S., Lo, S., Ma, J., Wang, W. (2014a). An agent-based microscopic pedestrian flow simulation model for pedestrian traffic problems. *IEEE Transactions on Intelligent Transportation Systems*, *15*(3), 992-1001.

Liu, Y., Wang, W., Huang, H. Z., Li, Y., & Yang, Y. (2014b). A new simulation model for assessing aircraft emergency evacuation considering passenger physical characteristics. *Reliability Engineering & System Safety*, 121, 187-197.

Luo, L., Fu, Z., Zhou, X., Zhu, K., Yang, H., Yang, L. (2016). Fatigue effect on phase transition of pedestrian movement: experiment and simulation study. *Journal of Statistical Mechanics: Theory and Experiment*, *2016*(10), 103401.

Luo, L., Fu, Z., Cheng, H., & Yang, L. (2018). Update schemes of multi-velocity floor field cellular automaton for pedestrian dynamics. *Physica A: Statistical Mechanics and its Applications, 491,* 946-963.

Moussaïd, M., Helbing, D., Theraulaz, G. (2011). How simple rules determine pedestrian behavior and crowd disasters. *Proceedings of the National Academy of Sciences*, *108*(17), 6884-6888.

Müller, K. (1981). *Zur Gestaltung und Bemessung von Fluchtwegen für die Evakuierung von Personen aus Bauwerken auf der Grundlage von Modellversuchen* (Doctoral dissertation).

Nagai, R., Fukamachi, M., & Nagatani, T. (2006). Evacuation of crawlers and walkers from corridor through an exit. *Physica A: Statistical Mechanics and its Applications*, *367*, 449-460.

National Standard of the People's Republic of China, GB 50096-2011. (2011). Design code for residential buildings.

National Standard of the People's Republic of China, GB 10000-88. (1988). Human dimensions of Chinese adults.

Paris, S., Pettré, J., Donikian, S. (2007, September). Pedestrian reactive navigation for crowd simulation: a predictive approach. In *Computer Graphics Forum* (Vol. 26, No. 3, pp. 665-674). Blackwell Publishing Ltd.

Pelechano, N., & Malkawi, A. (2008). Evacuation simulation models: Challenges in modeling high rise building evacuation with cellular automata approaches. *Automation in construction*, *17*(4), 377-385.

Schadschneider, A., & Seyfried, A. (2009). Validation of CA models of pedestrian dynamics with fundamental diagrams. *Cybernetics and Systems: An International Journal*, *40*(5), 367-389

Schadschneider, A., Klingsch, W., Klüpfel, H., Kretz, T., Rogsch, C., Seyfried, A. (2011). Evacuation dynamics: Empirical results, modeling and applications. In *Extreme Environmental Events* (pp. 517-550). Springer New York.

Seitz, M. J., & Köster, G. (2014). How update schemes influence crowd simulations. *Journal of Statistical Mechanics: Theory and Experiment*, 2014(7), P07002.

Seyfried, A., Steffen, B., Klingsch, W., & Boltes, M. (2005). The fundamental diagram of pedestrian movement revisited. *Journal of Statistical Mechanics: Theory and Experiment*, *2005*(10), P10002.

Seyfried, A., Passon, O., Steffen, B., Boltes, M., Rupprecht, T., & Klingsch, W. (2009). New insights into pedestrian flow through bottlenecks. *Transportation Science*, *43*(3), 395-406.

Song, W., Xu, X., Wang, B. H., Ni, S. (2006). Simulation of evacuation processes using a multi-grid model for pedestrian dynamics. *Physica A: Statistical Mechanics and its Applications*, *363*(2), 492-500.

Thompson, P. A., & Marchant, E. W. (1994). Simulex; developing new computer modelling techniques for evaluation. *Fire Safety Science*, *4*, 613-624.

Vicsek, T., Zafeiris, A. (2012). Collective motion. *Physics Reports*, *517*(3), 71-140.

Weidmann, U. (1992). Transporttechnik der fussgänger: Transporttechnische Eigenschaften des Fussgängerverkehrs (Literaturauswertung). IVT, Zürich.

Wirz, M., Franke, T., Roggen, D., Mitleton-Kelly, E., Lukowicz, P., & Tröster, G. (2013). Probing crowd density through smartphones in city-scale mass gatherings. *EPJ Data Science*, *2*(1), 5.

Weng, W. G., Pan, L. L., Shen, S. F., Yuan, H. Y. (2007). Small-grid analysis of discrete model for evacuation from a hall. *Physica A: Statistical Mechanics and its Applications*, *374*(2), 821-826.

Xu, X., Song, W. G., Zheng, H. Y. (2008). Discretization effect in a multi-grid egress model. *Physica A: Statistical Mechanics and its Applications*, *387*(22), 5567-5574.

Zhang, J., Song, W., Xu, X. (2008). Experiment and multi-grid modeling of evacuation from a classroom. *Physica A: Statistical Mechanics and its Applications*, *387*(23), 5901-5909.

Zhu, K., Yang, Y., Niu, Y., Fu, Z., & Shi, Q. (2017). Modeling pedestrian flow on multi-storey stairs considering turning behavior. *International Journal of Modern Physics C*, *28*(03), 1750034.